Enhanced charge collection via nanoporous morphology in polymer solar cells

Hang Ken Lee,[1] Ji Hye Jeon,[1] Dong Hwan Wang,[1] O. Ok Park,[1,a)] Jai-Kyung Kim,[2] Sang Hyuk Im,[3] and Jong Hyeok Park[4]
[1]*Department of Chemical and Biomolecular Engineering(BK21 Graduate Program), Korea Advanced Institute of Science and Technology, 335 Gwahangno, Yuseong-gu, Daejeon 305-701, Republic of Korea*
[2]*Center for Energy Materials Research, Materials Science and Technology Division, Korea Institute of Science and Technology (KIST), Seoul 136-791, Republic of Korea*
[3]*Korea Research Institute of Chemical Technology, 19 Singsungno, Yuseong-gu, Daejeon 305-600, Republic of Korea*
[4]*Department of Chemical Engineering, Sungkyunkwan University, Suwon 440-746, Republic of Korea*

(Received 23 December 2009; accepted 18 February 2010; published online 11 March 2010)

We demonstrated a simple and nonlithographic method that enlarges the active layer/metal electrode contact area in polymer solar cells by adding the thermal initiator 2,2′-azobisisobutyronitrile (AIBN) as a nanohole generating agent. From diffused light spectra and x-ray diffraction measurements, it is found that device performance enhancement comes not from a change in the charge carrier generation or transportation characteristics but from increased charge carrier collection due to the reduced contact resistance and shortened pathway to the electrode caused by enlarged interface area. © *2010 American Institute of Physics*. [doi:10.1063/1.3359425]

Converting solar energy into electricity using conjugated polymers has emerged as an alternative renewable energy source for low-cost, lightweight, large-area, and flexibility.[1] At present, conjugated polymers blended with a fullerene derivative which forms bulk heterojunction showed best performance around 4%–5% under AM 1.5 standard reference conditions.[4–10] In the bulk heterojunction structure, blended donor (D) and acceptor (A) materials form randomly interpenetrated network phases. To generate an external current, photogenerated free-charge carriers (electrons and holes) are transported toward the corresponding electrode and collected there. However, by such a random distribution of donor and acceptor materials, there is a charge trapping at bottlenecks and cul-de-sacs along the conducting path to appropriate electrodes.[2,3] To facilitate the charge transport, the active layer bulk morphology has been controlled by various methods including thermal/solvent/electrical annealing,[4,6,7] composition adjustment,[8] and addition of chemical additives.[9,10] In contrast, in comparison with the bulk morphology case, less attention has been paid on to the interface morphology between active layer and electrode which plays a key role in charge collection of the devices. Soft lithographic techniques such as replica molding or nanoimprinting have been applied to control of the active layer-electrode interface structure by enlarging the interface area.[11,12] This approach showed short conducting pathway without dead ends, reduced contact resistance, and ameliorated light absorption. However, lithographic methods require an extra procedure to fabricate a prepatterned mold and are hard to produce large area. In this letter, we introduce an alternative method that extends the interface area between active layer and metal electrode by introducing a nanoporous morphology using thermal initiator, 2,2′-azobisisobutyronitrile (AIBN), as a nanohole generating agent in the active layer. This method is mold-free and can be applied to a large area, therefore more cost-effective compared to lithographic methods.

Figure 1 presents a schematic diagram of the process flow of this approach. To fabricate polymer solar cells (PSCs), indium tin oxide glass was cleaned and then exposed to oxygen plasma for 10 min before use. A buffer layer poly(3,4-ethylene dioxythiophene):poly(styrene sufonate) (PEDOT:PSS) (Baytron P) was then spin-coated to a thickness of ~35 nm. After annealing the PEDOT:PSS films at 200 °C for 5 min, a photoactive layer composed of P3HT (Rieke Met. Inc.), PCBM (Nano-C) and AIBN (1:0.6:x in weight ratio, x ranges from 0 to 0.3) was spin-coated at 900 rpm for 5 s from chlorobenzene with 80 nm ± 5 nm thin films onto the precoated PEDOT:PSS layer. The prepared organic film was then thermally annealed at 105 °C for 10 min. AIBN is a typical initiator used in thermal polymerization, and dissociates into radicals above 65 °C to release stable nitrogen gas. Therefore during this annealing step, generated N_2 gas is released from active layer surface, leading to a nanoporous morphology. Generally, the half-life time of AIBN is expressed by following equation as follows:

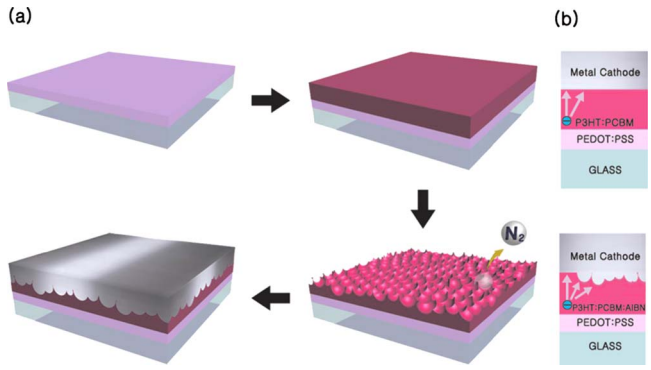

FIG. 1. (Color online) (a) Schematic fabrication flow of the nanoporous active layer applied polymer solar cell (b) (Top) Schematic diagram of a conventional and (Bottom) nanoporous active layer applied device.

a)Electronic mail: ookpark@kaist.ac.kr.

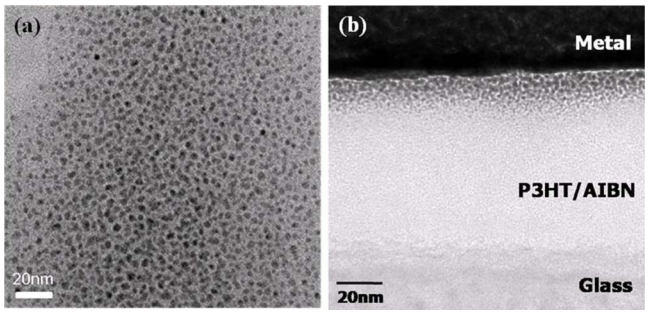

FIG. 2. (Color online) TEM images of P3HT/AIBN=1:0.1 film after heating at 105 °C for 5 min. (a) In plane. (b) Cross-section.

$$\log(t_{1/2}) = 7142\left(\frac{1}{T}\right) - 18.355T,$$

where, $t_{1/2}$: half-life time and T: temperature. According to this equation, $t_{1/2}$ at 105 °C is only 3 min, hence it can be believed that most of AIBN decomposed during the annealing procedure. The polymer chains of P3HT are stable against the radicals released from AIBN due to the rapid termination of radicals by mutual atomic recombination.[13,14] Finally LiF (0.6 nm) and Al(100 nm) electrodes were deposited under 5×10^{-7} torr as metal cathodes. The defined active area was 9 mm^2 and all procedures were performed in a N_2 gas-filled glove box. The current-density-voltage (J-V) curves were measured by a Keithley 2000 source-measure unit. The photocurrent was obtained under illumination from a Thermal Oriel solar simulator (AM 1.5G). The illumination intensity used was calibrated by a standard Si photodiode detector (Fraunhofer ISE, Certificate No. C-ISE269).

To confirm the nanoholes generated by AIBN decomposition, both in-plane and cross-sectional transmission electron microscopy (TEM) images were taken. Figure 2(a) shows an in-plane TEM image from P3HT/AIBN in optimal weight ratio of 1/0.1, which displayed the highest power conversion efficiency (PCE). This image clearly shows that 2–5 nm nanopores were formed by generation of N_2 gas throughout the film. However, as only nanopores created near the film surface can contribute to enlarge the interface area between active-layer and metal cathode, it is necessary to observe where the nanopores are located. Figure 2(b) shows the location of the nanopores within the film. This cross-sectional TEM image reveals that nanopores formed within 20 nm from the active-metal cathode interface and filled with evaporated Al ions well.

The device current density-voltage (J-V) characteristics under simulated air mass 1.5G illumination (100 mW/cm^2) with various AIBN blending ratios are shown in Fig. 3. For a reference device [Fig. 1(b) top], the PCE was 2.18% with a short-circuit current density (J_{sc}) of 6.6 mA/cm^2 and a fill factor (FF) of 52.4%. However, when AIBN was blended into the active layer with 0.05 and 0.1 wt % respect to P3HT, J_{sc} and FF value is increased so overall PCE was reached to 2.77% (with J_{sc} of 7.26 mA/cm^2 and FF of 59%), 3.10% (with J_{sc} of 7.61 mA/cm^2 and FF of 63.2%), respectively. These results suggest that charge collection loss decreases owing to the enlarged interface area between active layer and Al metal cathode resulted in reduced contact resistance and shortened pathway to electrode without dead ends [Fig. 1(b)]. Here, it is notable that PCE enhancement does not solely depend on an increase of J_{sc} but also an increase of FF.

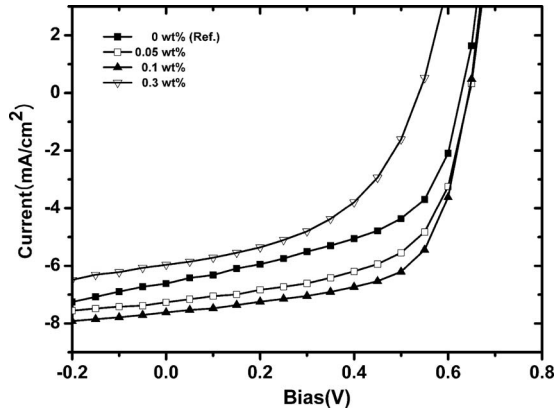

FIG. 3. Current/voltage characteristics of PSCs with different AIBN contents in P3HT/PCBM=1:0.6 active layer (in weight ratio) under illumination (simulated AM1.5G, 100 mW cm^{-2}).

Due to the efficient electron extraction, the charge recombination and leakage current are reduced and this is attributed to increase in FF. Over 0.1 wt % AIBN blended device, the PCE decreased to 1.53% (with J_{sc} of 5.96 mA/cm^2 and FF of 47.7%). After decomposition of AIBN, nonconducting residual materials remain in the active layer. It is speculated that this residual content hinders the charge transport when AIBN blended over 0.1 wt %. In addition, deteriorated charge transportation by adding AIBN [Fig. 4(b)] also counterbalances the enlarged interface area effect. In principle, the external photocurrent density is depends on the amount of generated charge carrier by photon absorption, photoge-

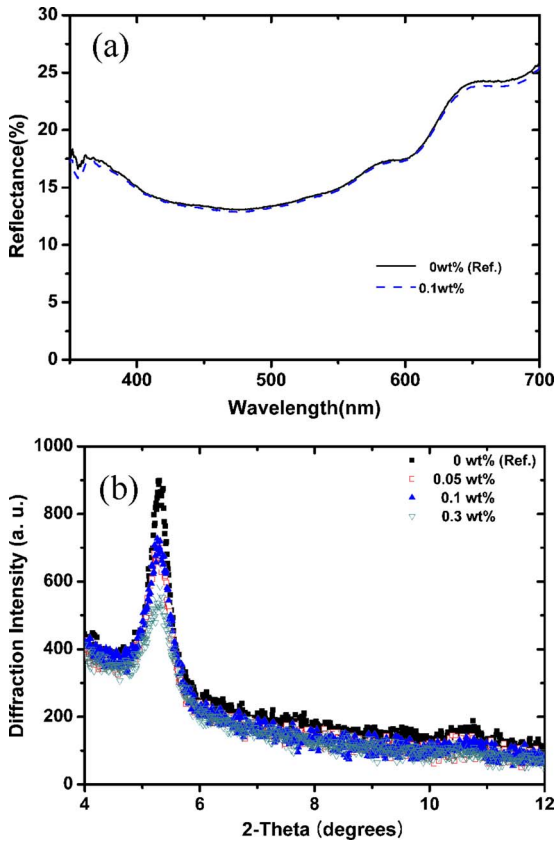

FIG. 4. (Color online) (a) Diffused reflectance spectra with and without AIBN in P3HT:PCBM active layer (b) x-ray diffraction of P3HT/PCBM/AIBN films with different AIBN contents in P3HT/PCBM=1:0.6 active layer (in weight ratio).

nerated charge carrier transport, and charge collection at the electrode. To evaluate the effect of an AIBN addition on these properties, diffused reflectance spectra and x-ray diffraction (XRD) were investigated.

Nanopores that are generated on an active layer-metal interface can act as a scattering media; therefore, light absorption in the active layer can be enhanced by extended light pathway. However, light absorption cannot be obtained directly because of deposited metal electrode, thus the diffused reflectance spectra were measured instead. In this method, the part of the incident beam that is scattered and reflected inside the device and returned to the surface is measured. Hence, the intensity of reflectance is proportional to the number of unabsorbed photons (lower reflectance indicates stronger absorption of incident light). Figure 4(a) shows the reflectance spectra with and without AIBN active layer. In this figure, there is no significant difference between with and without AIBN devices because nanopore size was too small to act as a scattering media for incident light.[15] From this, the effect on carrier generation can be excluded as a reason of increased J_{sc} and FF.

Figure 4(b) shows the XRD spectra with and without AIBN active layer. Mixing a third component into the active layer can change the self-organization property of electron donor P3HT. In Fig. 4(b), AIBN added active layer showed decreased intensity at $2\theta \approx 5°$, which means lower ordering compared to those without AIBN. This indicates that the mobility of the charge carrier in the P3HT films with AIBN added is decreased.[4] Although charge carrier transport is decreased, the device with AIBN showed improved performance as depicted in Fig. 3. This is one of the experimental evidence to demonstrate how the active layer-electrode interface structure is important for the generation of a photocurrent.

In summary, a simple and nonlithographic approach to broaden the contact area between organic/metal interfaces is demonstrated by incorporating AIBN into the active layer. After absorbing thermal energy, AIBN releases nitrogen gas from active layer surface, thus greatly increasing the interfacial area. In spite of the deteriorated carrier transport property of active layer by AIBN, device performance was improved by facilitated charge collection via reduced contact resistance and shortened pathway to electrode as a consequence of the enlarged interface area. In particular, the *efficient electron extraction* aided to decrease charge recombination, so FF as well as J_{sc} were attributed to improvement of PCE.

This work was supported by ERC grant of National Research Foundation of Korea (NRF) funded by the Korea Ministry of Education, Science, and Technology (MEST) [Grant No. R11-2007-045-01002-0(2009)] and KIST internal projects under contracts 2E20298. It was also partially supported by a WCU grant from MEST (Grant No. R32-2008-000-10142-0).

[1] S. Günes, H. Neugebauer, and N. S. Sariciftci, Chem. Rev. (Washington, D.C.) **107**, 1324 (2007).
[2] G. Yu, J. Gao, J. C. Hummelen, F. Wudl, and A. J. Heeger, Science **270**, 1789 (1995).
[3] F. Yang, M. Shtein, and S. R. Forrest, Nature Mater. **4**, 37 (2005).
[4] W. Ma, C. Yang, X. Gong, K. Lee, and A. J. Heeger, Adv. Funct. Mater. **15**, 1617 (2005).
[5] G. Li, V. Shrotriya, J. Huang, Y. Yao, T. Moriarty, K. Enery, and Y. Yang, Nature Mater. **4**, 864 (2005).
[6] G. Li, Y. Yao, H. Yang, and Y. Yang, Adv. Funct. Mater. **17**, 1636 (2007).
[7] F. Padinger, R. S. Rittberger, and N. S. Sariciftci, Adv. Funct. Mater. **13**, 85 (2003).
[8] J. M. Kroon, M. M. Wienk, W. J. H. Verhees, and J. C. Hummelen, Thin Solid Films **403-404**, 223 (2002).
[9] A. Pivrikas, P. Stadler, H. Neugebauder, and N. S. Sariciftici, Org. Electron. **9**, 775 (2008).
[10] K. C. Kim, J. H. Park, and O. O. Park, Sol. Energy Mater. Sol. Cells **92**, 1188 (2008).
[11] S.-I. Na, S.-S. Kim, S.-S. Kwon, J. Jo, J. Kim, T. Lee, and D. Y. Kim, Appl. Phys. Lett. **91**, 173509 (2007).
[12] J. H. Lee, D. W. Kim, H. Jang, J. K. Choi, J. Geng, J. W. Jung, S. C. Yoon, and H. T. Jung, Small **5**, 2139 (2009).
[13] S. W. Tong, C. F. Zhang, C. Y. Jiang, Q. D. Ling, E. T. Kang, D. S. H. Chan, and C. Zhu, Appl. Phys. Lett. **93**, 043304 (2008).
[14] T. H. Kim, S. H. Im, and O. O. Park, Appl. Phys. Lett. **87**, 221114 (2005).
[15] H. C. Van de Hulst, *Light Scattering by Small Particles* (Dover, New York, 1981).